Landscape and Urban Planning 215 (2021) 104198

Contents lists available at ScienceDirect

Landscape and Urban Planning

journal homepage: www.elsevier.com/locate/landurbplan

Assessing vegetation response to irrigation strategies and soil properties in an urban reserve in southeast Australia

V. Marchionni [a,*], S. Fatichi [b], N. Tapper [c], J.P. Walker [e], G. Manoli [d], E. Daly [e]

[a] School of Engineering, RMIT University, Melbourne, Australia
[b] Department of Civil and Environmental Engineering, National University of Singapore, Singapore
[c] School of Earth, Atmosphere, and Environment, Monash University, Melbourne, Australia
[d] Department of Civil, Environmental and Geomatic Engineering, University College London, London, UK
[e] Department of Civil Engineering, Monash University, Melbourne, Australia

HIGHLIGHTS

- Increasing tree cover makes irrigation essential during a prolonged drought.
- Irrigation helps alleviate water competition between different vegetation types.
- Soil type strongly affects the water status and competitiveness of vegetation.

ARTICLE INFO

Keywords:
Urban green spaces
Remnant vegetation
Irrigation
Stormwater harvesting
Ecohydrological modeling

ABSTRACT

Increasing urban green spaces and canopy cover requires careful planning of irrigation strategies, especially in arid and semiarid areas. This study investigates how vegetation cover and irrigation affect the water balance and vegetation productivity of a small urban reserve in the Melbourne metropolitan area, Australia. Using a mechanistic ecohydrological model, a series of numerical experiments were carried out for the period 1999–2018, which included a prolonged drought. Results indicated that irrigation played an essential role in helping both trees and grass productivity by increasing soil moisture and vegetation water access during the drought. With 10% tree cover, grass benefitted more than trees by increasing irrigation, and trees coped well with drought even without additional water. However, trees strongly relied on irrigation to maintain productivity when tree cover increased, highlighting the need for a sustainable balance between increasing urban greening and water conservation. Differences in soil properties and rooting strategies were also found to strongly modify the need for irrigation and the competition for water. These results provide quantitative insights on how increasing tree cover and vegetation diversity may impact irrigation requirements, highlighting the key role of mechanistic numerical models to support urban planners in the evaluation and design of urban green spaces.

1. Introduction

Green spaces are increasingly considered crucial components of the urban environment, helping cities to become more resilient to the negative impacts of both urbanization and climate change (Luederitz et al., 2015; Livesley, McPherson, & Calfapietra, 2016; Marchionni, Revelli, & Daly, 2019; Meili et al., 2020). Urban green spaces are recognized to provide natural cooling and support stormwater management (Spronken-Smith & Oke, 1998; Gill, Handley, Ennos, & Pauleit, 2007; Broadbent, Coutts, Tapper, & Demuzere, 2018), deliver essential ecosystem services for community health and well-being (Chiesura, 2004), and offer habitat for urban biodiversity (Elmqvist et al., 2015; Lepczyk et al., 2017; Tulloch, Barnes, Ringma, Fuller, & Watson, 2016). As a result, government authorities and urban planners worldwide are committed to increasing tree canopy cover, while preserving existing urban green spaces to provide healthy and sustainable urban settings. For example, councils across the Melbourne metropolitan area (Australia) are implementing actions to increase the tree canopy cover by 40% by 2040 (Melbourne, 2012). Similar targets were set through the London Environmental Strategy (i.e., increasing green cover by 50% by

* Corresponding author.
E-mail address: valentinamarchionni@gmail.com (V. Marchionni).

https://doi.org/10.1016/j.landurbplan.2021.104198
Received 18 January 2021; Received in revised form 9 July 2021; Accepted 16 July 2021
Available online 28 July 2021

2050) and the Million Trees initiatives in New York City and Los Angeles (e.g., McPherson, Simpson, Xiao, & Chunxia, 2008). The importance of these greening policies has been further highlighted by the enhanced appreciation and demand for green spaces during the recent COVID-19 pandemic (Kleinschroth & Kowarik, 2020).

In urban areas, vegetation is generally subjected to biophysical and ecological conditions that are different from rural and natural environments, with respect to soil and micro-meteorological conditions in particular (Calfapietra, Peñuelas, & Niinemets, 2015). Therefore, to provide the expected ecosystem services, urban vegetation often needs to be managed to remain healthy and productive in spite of often unfavorable growing conditions, such as high temperatures and low soil moisture (Roberts, 1977; Sieghardt et al., 2005). Irrigation may play a crucial role in supporting ecosystem health and biodiversity in cities. Especially in seasonally dry climates, the coexistence of different vegetation types, such as trees, shrubs, and grass, as well as remaining native vegetation and introduced non-native species may create unique biotic communities highly dependent on water, thus needing irrigation to be sustained (McCarthy & Pataki, 2010; Pataki et al., 2011). In addition, hotter temperatures and rainfall reduction increase the competition among vegetation types, with soil characteristics playing a crucial role in the water status of vegetation, as shown in Marchionni et al. (2020).

The need for irrigation is becoming increasingly important under a rapidly changing climate, as more frequent and severe extremes, such as droughts and heatwaves, increase the risk of plant mortality and reduce productivity (Soylu, Istanbulluoglu, Lenters, & Wang, 2011; Allen, Breshears, & McDowell, 2015; Breshears et al., 2005 Mcdowell et al., 2016; Qiu et al., 2019), as well as exacerbate the pressure on water resources (Flörke, Schneider, & McDonald, 2018). In these conditions, normal irrigation amounts may also be insufficient to maintain plant functioning during hotter droughts leading to vegetation losses (Quesnel, Ajami, & Marx, 2019; Miller, Alonzo, Roberts, Tague, & McFadden, 2020; Allen, Roberts, & McFadden, 2021). The use of recycled wastewater and captured stormwater for urban vegetation irrigation is a valuable option to sustain vegetation while relieving the pressure on potable water resources (Nouri, Borujeni, & Hoekstra, 2019; Livesley, Marchionni, Cheung, Daly, & Pataki, 2020). Other actions may include the choice of appropriate irrigation practices, irrigation-scheduling depending on plant water demands, and water sensitive landscape designs (Pataki et al., 2011; Volo, Vivoni, Martin, Earl, & Ruddell, 2014; Litvak & Pataki, 2016; Breyer, Zipper, & Qiu, 2018). For instance, McCarthy, Pataki, and Jenerette (2011) suggested the use of the water-use efficiency (WUE) factor (i.e., the ratio of carbon assimilated by plants and water lost through transpiration) to select species that maximize productivity while conserving water.

These issues are particularly relevant in southeast Australia, where over the past two decades two of the worst droughts in the historical record have occurred, i.e., the Millennium Drought (2001–2009) and the recent drought (2017–2020) (De Kauwe et al., 2020). The Millennium Drought resulted in below median rainfall when compared to the previous century, contributing to the enforcement of severe water restrictions in most major cities, as well as reductions in vegetation biomass and major bushfire events in 2003 and 2009 (van Dijk et al., 2013; Sawada & Koike, 2016). The recent drought occurred against the background of increasing air temperature (i.e., droughts are getting hotter), with 2019 the hottest and driest year on record; this led to a significant amount of tree stress and the 2019/20 Black Summer bushfire disaster (Abram et al., 2021).

For Melbourne, more than a decade of severe drought and water restrictions provided the opportunity to implement a water sensitive urban design (WSUD) approach for a more integrated and sustainable water management (Low et al., 2015). This included the development of stormwater harvesting projects to reuse stormwater runoff, thus providing alternative water sources for irrigating urban green spaces (Martire, 2018). The use of this water can help buffering the decline in vegetation productivity due to the prolonged drought and periods of extreme heat (Marchionni et al., 2020). An example is the stormwater harvesting system at Fitzroy Gardens, which is the largest in the City of Melbourne and provides up to 69000 m^3 of water every year for irrigation, thus decreasing the use of potable water for irrigating the gardens by 59% (Wallace, 2014).

The aim of this study was to assess the effectiveness of different irrigation strategies in supporting coexisting types of vegetation at Napier Park, which is an urban reserve hosting native vegetation in the Melbourne metropolitan area in southeast Australia. With an extensive irrigation system covering about 85% of the reserve, Napier Park is an example of the implementation of a stormwater harvesting and reuse system to irrigate urban green spaces to sustain ecosystem dynamics, while retaining water in the urban landscape. A series of numerical experiments were carried out using the mechanistic ecohydrological model Tethys-Chloris (T&C) to investigate different irrigation and vegetation cover scenarios, as well as the impacts of the Millennium Drought (2001–2009). Extensively used since 2012, the T&C model has been already applied to reserves with similar ecosystems in Marchionni et al. (2020) because of its capability to represent average reserve-scale processes. The specific questions addressed are as follows: (1) How do increasing tree cover and irrigation rates affect tree transpiration and vegetation productivity? (2) How can different vegetation types (trees-shrubs-grass) coexist and is this coexistence threatened in dry periods? (3) How do soil properties affect competition among vegetation types? Results from this study improve the understanding of how urban reserves and relatively large urban green spaces can be effectively managed ensuring both vegetation productivity and water savings.

2. Methods

2.1. Site and data description

A small urban reserve, Napier Park (37.74°S, 144.91°E), located in the Melbourne metropolitan area in southeast Australia (Fig. 1a), was selected as a case study (Marchionni, Guyot, Tapper, Walker, & Daly, 2019). The climate of the area is Mediterranean (Cfa in the Köppen classification) with an average annual rainfall of 522 ± 113 mm y^{-1} over the period 2009–2018 (BOM station Melbourne Airport, No. 086282; 37.67° S, 144.83° E; 113 m AHD; *http://www.bom.gov.au/watl/eto/*).

The reserve, managed by a local council, is a 4 ha remnant plain grassy woodland home to a valuable population of *Eucalyptus Camaldulensis* with a number of significant *Eucalyptus Melliodora*. The tree stand density is about 217 trees per hectare, with a mean diameter at breast height (DBH) of 210 mm. Texture-contrast (duplex) soils cover the entire area of the reserve, with the soil profile consisting of a sandy silt (up to 0.4–0.6 m), overlaying a heavy clay (up to 1.8 m) followed by sandy silt again. The water table is estimated to be between 10 and 20 m below the ground surface.

An extensive irrigation system was implemented in 2016, covering about 85% of the reserve ($\sim$ 3.4 ha), to alleviate the visible decline in vegetation health. Specifically, stormwater is harvested from an upstream catchment of about 16.3 ha, and used for irrigation with the intent to recharge the clay subsoil during the wetter months, thereby providing a source of water for the remnant trees in the dryer months (Fig. 1b). The stormwater harvesting and irrigation system was designed to include a vegetated swale, which also provides passive treatment of stormwater flows while re-establishing an ephemeral waterway that naturally occurred before the area was urbanized. The vegetated swale conveys stormwater from the urbanized catchment into an underground storage tank (115 m^3); the water is pumped from the tank at the end of each stormwater flow event to supply a reticulated distribution system throughout the reserve. Recharge bores (30 cm diameter and 45 cm depth) are used as part of the irrigation distribution network to promote direct infiltration into the clay layer at 50 cm depth. The irrigation strategy aims at increasing the volume of water received by the reserve of an amount equivalent to lengthening the duration of each rainfall

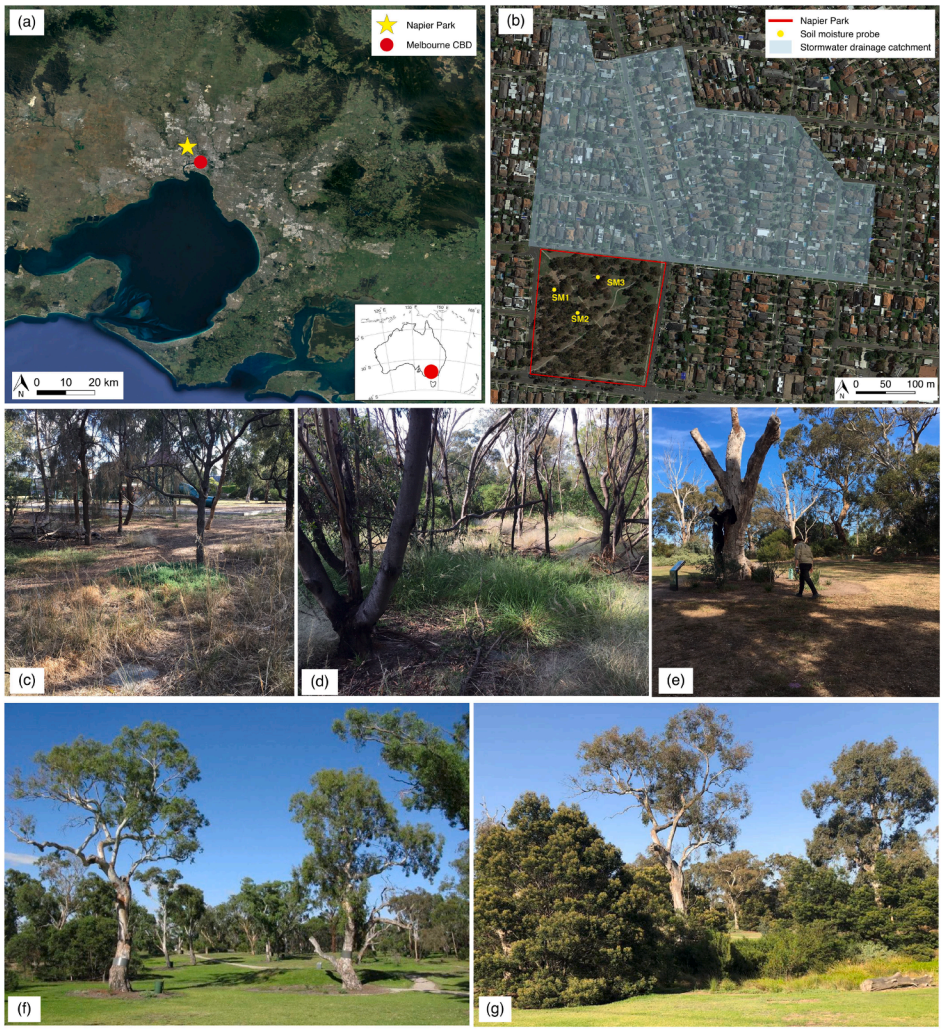

Fig. 1. (a) Location of the study site with respect to the Melbourne Central Business District (CBD). (b) Locations of the contributing stormwater drainage catchment with respect to the study site and soil moisture sensors. Images of the locations where the soil moisture probes were installed: (c) SM1, (d) SM2, (e) SM3. A comparison of the vegetation cover in (f) 2012, before irrigation was implemented, and (g) 2019, after a few years of supplementary watering.

event up to 3 h.

Since irrigation started in 2016, spontaneous revegetation of low and medium height plants has occurred in large areas of the reserve (Figs. 1f and 1g). However, it is difficult to determine whether this is a direct result of irrigation or the return of rainfall patterns closer to the long-term averages in recent years (i.e., 2012–2017). Measurements of soil volumetric water content were collected at three locations across the site (Fig. 1b) from September 2014 to June 2018 using fully encapsulated soil water capacitance probes (Drill & Drop by Sentek). The probes measure soil volumetric water content through sensors spaced at 10 cm intervals from the surface to a depth of 120 cm. Soil water profiles were recorded every 15 min and accessed through the online software IrriMAX Live. Long-term (July 1999 - June 2018) meteorological data, including rainfall, air temperature, relative humidity, wind speed, and solar radiation are available every 30 min from the Bureau of Meteorology (BOM) weather stations network (BOM station Melbourne Airport).

2.2. Modeling

2.2.1. Tethys-Chloris model

Model simulations were carried out using the Tethys-Chloris (T&C) model (e.g., Fatichi, Zeeman, Fuhrer, & Burlando, 2014; Manoli et al., 2018 Mastrotheodoros et al., 2019), which simulates essential components of the hydrological and carbon cycles, resolving energy, water, and carbon fluxes at the land surface at an hourly time step. The model combines equations for the energy and water balance budgets, accounting for plant life-cycle processes, such as photosynthesis, carbon allocation, and tissues turnover, which modulate the exchange of water and carbon between land and atmosphere. A detailed description of the mathematical formulation of the model components (i.e., energy and water fluxes, unsaturated–saturated zone interactions, subsurface-surface flows, and the processes affecting the carbon balance of vegetation) can be found in Fatichi, Ivanov, and Caporali (2012). Further details about the model are also presented in the Supplementary Material (Text S1). Meteorological inputs required for forcing T&C include rainfall, air temperature, relative humidity, wind speed, solar radiation, atmospheric pressure, cloud cover or longwave radiation, and atmospheric CO_2 concentration. Soil moisture dynamics are described by the one-dimensional Richards equation (Richards, 1931) for the vertical flow of water in the variably saturated soil column. T&C further accounts for biophysical and biochemical vegetation attributes using modules to simulate plant-related processes, such as photosynthesis, phenology, carbon pool dynamics, and tissue turnover (Fatichi et al., 2014; Fatichi & Pappas, 2017; Manoli, Ivanov, & Fatichi, 2018). Vegetation species diversity can be represented by aggregating species into Plant Functional Types (PFT). In this study, three PFTs were used to account for the coexistence of trees, grass, and shrubs. The model can

consider horizontal composition of vegetation patches; in particular, the land cover composition accounts for the area occupied by each vegetation type. Non-vegetated surfaces (i.e., bare soil) can also be taken into account. T&C simulates a number of ecohydrological variables including transpiration, soil evaporation, evaporation from interception, deep drainage (i.e., recharge), runoff, and profiles of soil moisture. It further simulates vegetation gross and net primary production, plant water stress and Leaf Area Index (LAI). Plant water stress is indicated with a factor, β, that expresses how the root integrated water potential departs from plant physiological thresholds characterizing incipient water stress. A reduction of β from 1 (unstressed conditions) affects plant photosynthesis, carbon allocation, and can trigger leaf shedding.

2.2.2. Model setup and parameter estimation

While different species and their spatial distribution can be accounted for, the urban reserve here was represented as a one-dimensional vertical system, i.e., without accounting for micro-topographic conditions and spatial variability of the soil properties over the site. This simplification of Napier Park is consistent with its small and homogeneous area and soil texture (i.e., soil is mostly clayey below 40 cm across the whole area, therefore significant lateral fluxes of water are unlikely), and allows an aggregated representation of reserve-scale ecohydrological processes as well as their response to different scenarios. The vertical soil domain was assumed to be limited to 1.8 m for a total of 20 discretization layers. The soil vertical layers have thicknesses that increases with depth, starting from 0.01 m at the surface. Free-drainage conditions were assigned at the bottom of the soil column.

Consistent with observations from the investigation works between March and April 2010, the soil profile was modeled as a sandy silt (up to 0.4 m) overlaying a heavy clay (between 0.4 and 1.8 m) (Table 1). The specific soil hydraulic properties were obtained through the *van Genuchten* model (Van Genuchten, 1980); the soil hydraulic parameters were manually adjusted during calibration, as discussed in Section 3.1.

Vegetation parameters (Table 2) were chosen based on literature and previous model applications (Fatichi & Pappas, 2017; Marchionni et al., 2020). In particular, two PFTs (i.e., grass and trees) were considered covering 80% and 10% of the reserve, respectively, with the remaining 10% considered as bare soil. An additional PFT (tall shrubs) was included for the scenario analysis, as described in Section 2.2.3. These vegetation fractions were based on local observations of the areas in which soil moisture profiles were monitored, as shown in Fig. 1c-e. To describe the root depth distribution, a linear dose–response profile was used (Collins & Bras, 2007). This required specification of the rooting depths that contain 50% and 95% of fine root biomass ($Z^{R,50}$ and $Z_{R,95}$).

Soil hydraulic parameters and root depth were manually calibrated to reproduce the average soil water dynamics across the site (Fig. 1b) using the data collected between September 2014 and December 2015 (before the start of irrigation). The ability of the model to reproduce soil water dynamics at the site was then confirmed for the 12 month period between January 2016 and December 2016, when irrigation was applied. The atmospheric forcing consisted of hourly observations of meteorological data from the nearby BOM Melbourne Airport weather station. Soil moisture and vegetation carbon pool initial conditions for the calibration simulations were generated by running a 1 year spin-up simulation starting from soil moisture conditions coinciding with field capacity at the bottom of the clay layer and an equilibrium profile (zero-flux) in the rest of the soil domain.

Table 1
Main soil parameters used in the simulations.

Depth (m)	Soil Type	*van Genuchten* coefficients (θ_s, θ_r, α, n)[a]	Saturated hydraulic conductivity (k^s; mm h^{-1})[b]
0.0–0.4	Sandy Silt	0.30, 0.09, 0.020 mm^{-1}, 1.7	k^s=-15.39 ln(z)+115.43
0.4–1.8	Clay	0.57, 0.20, 0.0006 mm^{-1}, 1.1	
0.0–0.4	Sandy Silt	0.30, 0.09, 0.020 mm^{-1}, 1.7	k^s=-6.93 ln(z)+95.96
0.4–1.8	Sandy Loam	0.41, 0.06, 0.008 mm^{-1}, 1.1	

[a] Carsel and Parrish (1988).
[b] k^s was assumed to be decreasing with depth (z, mm; positive downward) according to a logarithmic law, which was derived starting from the values of k^s obtained in the calibration for the various soil texture classes, i.e., 80 (Sandy Silt) and 0.10 (Clay) mm h^{-1}. For the sandy loam layer, k^s was assumed equal to 44 mm h^{-1} (Carsel & Parrish, 1988).

Table 2
Main vegetation parameters used in the simulations.

Parameter	Unit	Trees	Tall Shrubs	Grass
$Z_{R,50}$	m	0.50	0.20	0.15
$Z_{R,95}$	m	1.60	0.60	0.30
h^c	m	20.00	10.00	0.10
a_1	-	8.00	6.00	7.00
ψ_{S2}	MPa	−0.10	−0.10	−0.07
ψ_{S50}	MPa	−1.50	−1.50	−0.15
S^L	m^2/gC	0.009	0.012	0.016
r	gC/gN/d	0.042	0.036	0.038
$A_{L,cr}$	d	365	730	180
d_{mg}	d	20	15	20
T_{rr}	gC/m^2/d	1.00	0.40	2.50
L_{tr}	-	0.80	0.50	0.40
ϵ_{ac}	-	0.60	0.80	0.50
$1/K_{lf}$	d	40	50	40
$V_{c,max25}$	-	45	62	54
r_{JV}	-	2.00	2.00	2.10

$Z_{R,50}$: root depth 50 percentile, $Z_{R,95}$: root depth 95 percentile, h^c: canopy height, a_1: empirical parameter connecting stomatal aperture and net assimilation, ψ_{S2}: water potential at 2% stomatal closure, ψ_{S50}: water potential at 50% stomatal closure, S_L: specific leaf area, r: respiration rate at 10°C, $A_{L,cr}$: critical leaf age, d_{mg}: days of maximum growth, T_{rr}: translocation rate from carbohydrate reserve, L_{tr}: leaf to root biomass maximum ratio, ϵ_{ac}: parameter for allocation to carbon reserves, $1/K_{lf}$: dead leaf fall turnover, $V_{c,max25}$: maximum Rubisco capacity at 25°C leaf level, r_{JV}: scaling J_{max}- $V_{c,max}$.

2.2.3. Scenarios

A series of numerical experiments were designed to investigate the effects of increasing tree cover and irrigation rates on hydrological fluxes and vegetation productivity. Simulations were carried out using meteorological inputs from 1 July 1999 to 30 June 2018 observed at the BOM Melbourne Airport weather station.

Different tree cover percentages (i.e., 10%, 20%, and 30%) were investigated. An additional scenario was considered to account for the coexistence of trees (20%), tall shrubs (20%), and grass (50%) in areas of the reserve where spontaneous revegetation occurred mainly as low and medium height vegetation. The coexistence of trees, shrubs, and grass coverage was obtained by decreasing the percentage of grass cover while the percentage of bare soil (i.e., 10%) was maintained constant throughout all simulations, as shown in Table 3.

According to the design of the existing irrigation system at Napier

Table 3
Numerical experiments used for testing the effects of irrigation scenarios for different vegetation cover. The annual average of the additional water to the site is also specified for each irrigation scenario.

Scenario Code	Vegetation (%)				Irrigation (mm y^{-1})			
	Trees	Shrubs	Grass	Bare Soil	NA	+1 h	+2 h	+3 h
T10	10	0	80	10	0	98	197	295
T20	20	0	70	10				
T30	30	0	60	10				
S20	20	20	50	10				

Park, water was applied at a depth of 50 cm below the ground surface. Three different scenarios with irrigation of 0.5 mm h^{-1} after each rainfall event with irrigation lasting 1, 2, and 3 h were imposed for an annual average of additional rainfall to the site of about 98, 197, and 295 mm, respectively. During the drought period there were still rainfall events (although rare) that allowed implementing such irrigation strategy in our scenarios. A further scenario with no irrigation was also considered, for a total of four scenarios for each vegetation cover composition (Table 3).

To investigate the effect of soil properties on the vegetation response to irrigation, a sandy loam layer was considered instead of clay (Table 1) with respect to two different vegetation covers (10% trees, 10% bare soil, and 80% grass; 20% trees, 10% bare soil, 20% shrubs, and 50% grass) for all irrigation scenarios.

Soil moisture and vegetation carbon pool initial conditions were generated by running a spin-up simulation of 19 years, starting from the soil at field capacity at the bottom of the clay layer and an equilibrium profile in the rest of the soil column.

3. Results

3.1. Model calibration and testing

Fig. 2 shows observed and simulated soil water dynamics in the first 1.2 m of the soil domain in the periods selected for calibration (16 month period) and confirmation (12 month period), after manually adjusting soil hydraulic properties (Table 1) and root depths (Table 2).

The soil hydraulic parameters were homogeneous in the vertical direction within each soil texture class, except for the hydraulic conductivity at saturation (k_s), which was assumed to decrease with depth (z, positive downward) following a logarithmic profile. A specific equation was derived by fitting a logarithmic function to the values of k^s for the two soil texture classes (Table 1).

Overall, the model captured the behavior of the soil water dynamics averaged across the two soil layers. In the top soil layers, i.e., 0–40 cm, soil water dynamics were generally well captured by the model (R^2 = 0.72 and RMSE = 0.022 m^3m^{-3}), although soil moisture appeared to be slightly underestimated in some periods. At depths of 40–120 cm, soil moisture did not present large fluctuations and the slightly out of phase seasonal cycle of the model caused a lower R^2 of 0.32. However, the magnitude of soil moisture and its fluctuations remained low (RMSE = 0.018 m^3m^{-3}). The RMSE values for all the soil layers were below 0.04 m^3m^{-3} that often represents observation uncertainty, and it is considered acceptable for soil moisture modeling (Entekhabi et al., 2014).

3.2. Vegetation cover and soil scenarios

3.2.1. Water balance

The simulated effects of different vegetation cover and irrigation scenarios on the water balance components are shown in Fig. 3, expressed as mean values of the 19 years analyzed.

The average total evapotranspiration strongly increased with the percentage of tree cover, showing an increase of +26% with 30% of tree cover compared to the scenario with 10% of tree cover irrespective of the irrigation scenario (Fig. 3a). This is mainly linked to an increase in the tree transpiration of about +170% (Fig. 3c). Irrigation was found more beneficial for grass transpiration than tree transpiration, due to its shallower roots. However, when the 30% tree cover scenario was considered, trees were found to benefit from irrigation by increasing their transpiration by about 6% with a +1 h irrigation scenario compared to the no irrigation scenario (Fig. 3c, green bars). Both irrigation and vegetation cover slightly affected evaporation from bare soil and from water intercepted by the canopy (Fig. 3d), with an increase in evaporation from bare soil by about 15% in the +3 h irrigation scenario compared to the no irrigation scenario, regardless of the vegetation cover.

Both leakage, i.e. the water percolating from the bottom of the soil domain, and runoff decreased with increasing tree cover, and significantly increased with irrigation (Figs. 3e and 3f). Specifically, results showed an average reduction in leakage of −71% with the 30% of tree cover compared to the scenario with 10% of tree cover without irrigation. Leakage increased considerably as a result of irrigation, especially in the 30% tree cover scenario; this occurred because a greater amount of water into the clay layer did not enhance tree transpiration. The presence of shrubs led to more complex dynamics associated with the competition for soil water resources and consequently more variable soil moisture profiles; this resulted in tree transpiration being always below the shrubs transpiration despite both having 20% of the areal cover. Grass transpiration also decreased considerably (-64% regardless of the irrigation scenario) when compared to the 30% tree cover scenario, even

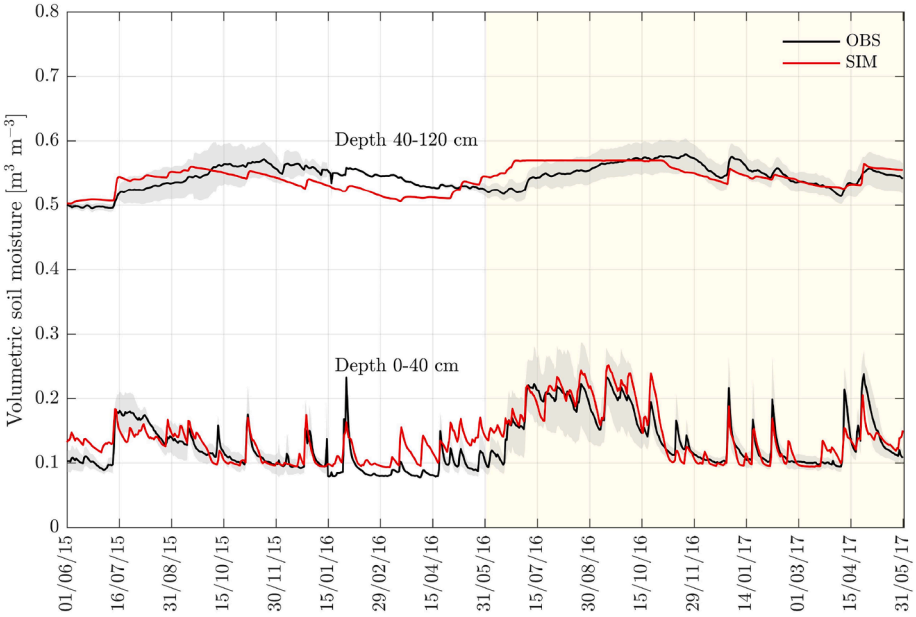

Fig. 2. Simulated and observed volumetric soil moisture in the calibration and confirmation (highlighted in yellow) periods averaged over the depths of 0–40 and 40–120 cm; observed volumetric soil moisture is represented as the mean values ± SD (grey areas) of the three probes used in the analysis, i.e., SM1, SM2, and SM3.

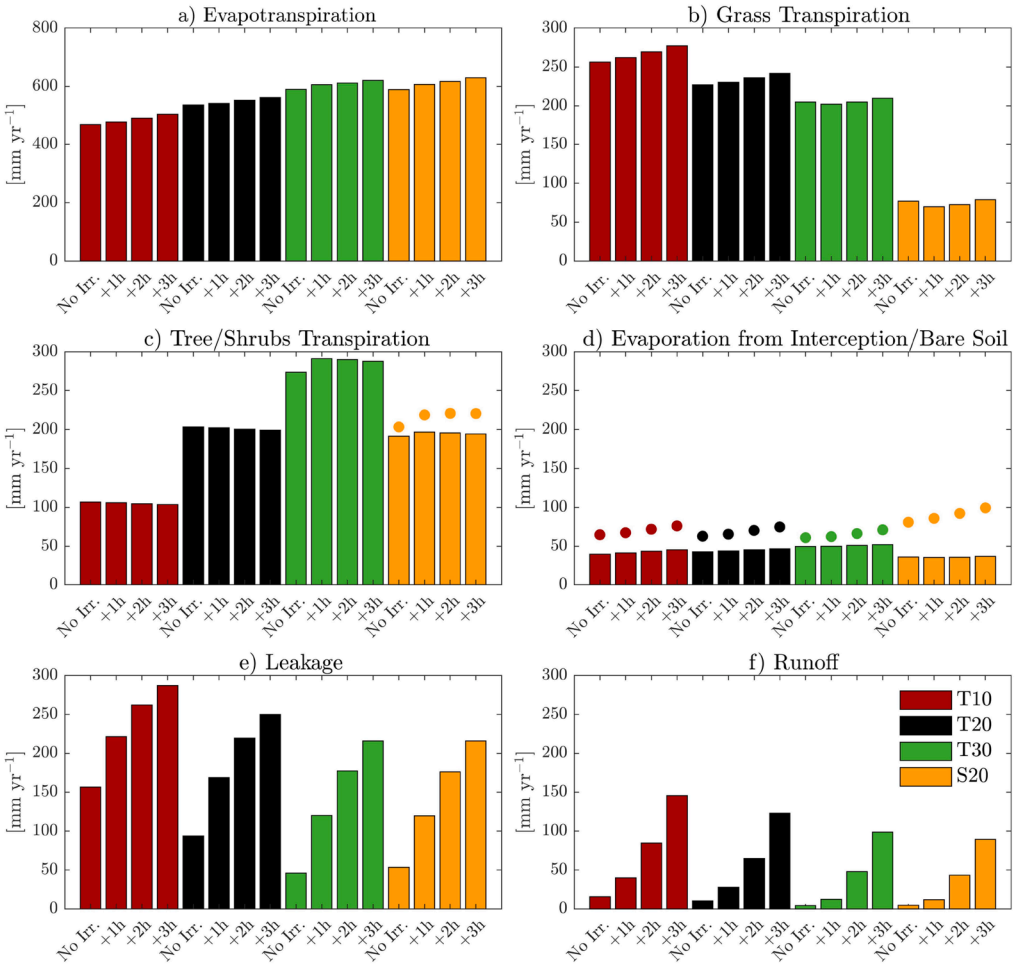

Fig. 3. Simulation results averaged over the 19-year period (July 1999-June 2018) illustrating the sensitivity of water balance components to vegetation cover scenarios (i.e., 10% (T10; red), 20% (T20; black), and 30% (T30; green) tree cover as well as 20% trees, 50% grass, and 20% shrubs cover (S20; orange)), and irrigation scenarios (i.e., No Irrigation, +1 h, +2 h, and +3 h). (a) Evapotranspiration, (b) Grass transpiration, (c) Trees (bars) and shrubs (dots) transpiration, (d) Evaporation from interception (bars) and bare soil (dots), (e) Leakage from the bottom of the soil domain, and (f) Runoff.

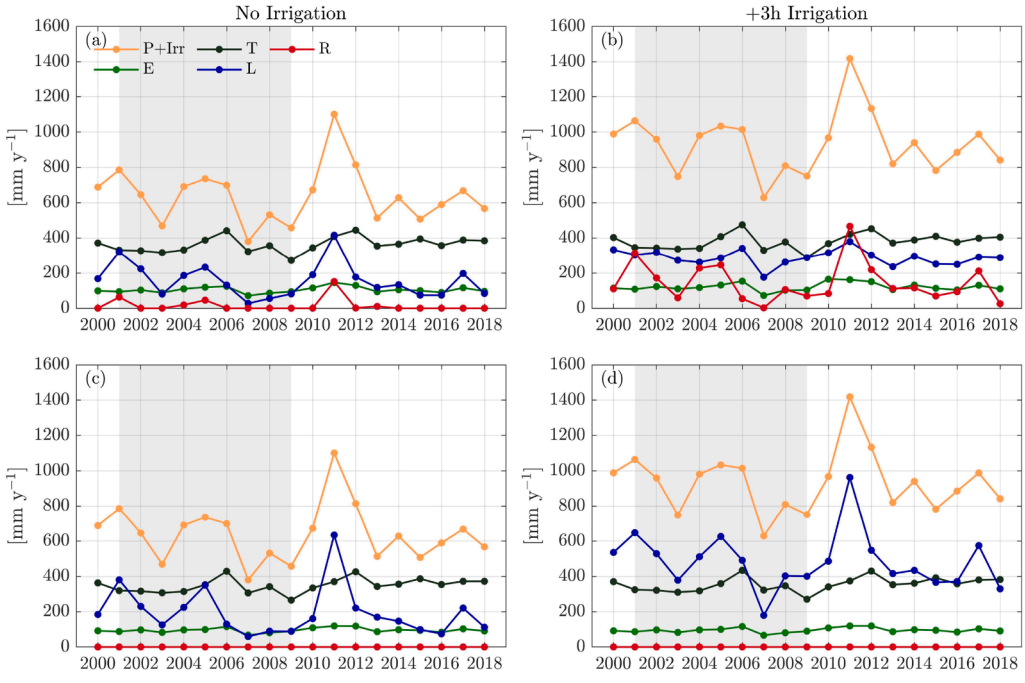

Fig. 4. Simulation results for the 19 year period (July 1999-June 2018) showing annual values of the water balance components, i.e., rainfall and irrigation (P +Irr), evaporation (E, i.e., evaporation from interception by canopy and ground evaporation), transpiration (T, i.e., grass and tree transpiration), leakage from the bottom of the soil domain (L), and runoff (R). Results correspond to the 10% tree cover scenarios for no irrigation (left column) and +3 h irrigation scenarios (right column) with (a, b) a clay layer and (c, d) a sandy loam layer at the bottom of the soil (0.4–1.8 m). Grey regions indicate the period of the Millennium Drought.

though grass areal covers in the two scenario slightly differ, i.e., 50% for the trees-shrubs-grass scenario and 60% for the 30% tree cover scenario.

Soil properties and bottom-free drainage conditions strongly affected runoff formation. In particular, without irrigation, runoff was equal to zero in most years except during very wet years (e.g., 2011), as shown in Fig. 4a for the 10% tree cover scenario. When a +3 h irrigation scenario was considered, substantial saturation excess runoff (and leakage) losses occurred due to the modest changes in tree transpiration with increasing irrigation (Fig. 4b). Different soil water-vegetation dynamics were found when a sandy loam layer below 0.4 m was considered instead of clay for both vegetation covers. Specifically, for the scenario with 10% of tree cover and without irrigation, even though tree transpiration did not increase, grass transpiration slightly decreased by about −6% (Fig. 4c). With the +3 h irrigation scenario, tree transpiration increased by +5%, whereas grass transpiration decreased on average by about −11% (Fig. 4d). Overall, due to the favored drainage in the coarser texture soil, runoff was also absent during wet years and leakage increased quite significantly in all scenarios, i.e., +28% for the scenario with no irrigation, +31% for the scenario with +1 h irrigation, +45% for the scenario with +2 h irrigation, and +66% for the scenario with +3 h irrigation.

Soil properties considerably modified the effects of both irrigation and vegetation cover on the vertical distribution of soil moisture (Fig. 5). The high water holding capacity of clay soil played a crucial role in maintaining high levels of soil moisture in all vegetation cover scenarios (Fig. 5a). When a sandy loam soil below 0.4 m was considered, the storage capacity was found inadequate to supply moisture to the woody plants even in the 10% tree cover scenario; additionally, increasing competitiveness when shrubs are included affected the water content profiles (Fig. 5b).

3.2.2. *Vegetation productivity*

The simulated effects of vegetation cover and irrigation scenarios on vegetation productivity are shown in Fig. 6 with respect to the 10%, 20%, and 30% tree cover, as well as for the scenario that accounts for the coexistence of trees (20%), shrubs (20%), and grass (50%). Gross primary productivity (GPP), leaf area index (LAI), and plant water stress factor (β) are used as variables to represent productivity, plant structure, and the risk of plants to wilt, respectively. They are expressed as mean values of the 19 years analyzed and in terms of unit of vegetated area to compare the results irrespective of the percentages of tree and grass covers (i.e., to obtain ecosystem GPP, the different fractional contributions must be weighted).

Results suggest that, overall, changes in vegetation cover and irrigation regime had more pronounced impacts on grass productivity than on tree productivity. The latter was marginally affected by the increased tree cover, only showing a small decrease in the 30% tree cover scenario (-5%) and in the trees-shrubs-grass scenario (-3%) (Fig. 6a). Grass showed overall higher GPP with increased tree cover because of reduced competition for water uptake at shallow depths (+11% on average with 30% of tree cover compared to the scenario with 10% tree cover; Fig. 6b). When the coexistence of trees (20%), shrubs (20%), and grass (50%) was taken into account, grass showed an overall reduction in GPP by about −50% over the entire period of analysis across all irrigation scenarios (Figs. 6b). Similar patterns were found in terms of LAI for both grass and trees, with small variations of LAI for trees across all scenarios (Figs. 6c and 6d).

Overall, trees coped well with the drought in the 10% tree cover scenario, but they appeared more stressed in the 30% tree cover scenario, as drought intensified between 2007 and 2009, reaching the highest plant water stress (i.e., $\beta = 0.90$) in 2007 (Fig. 7e). Conversely,

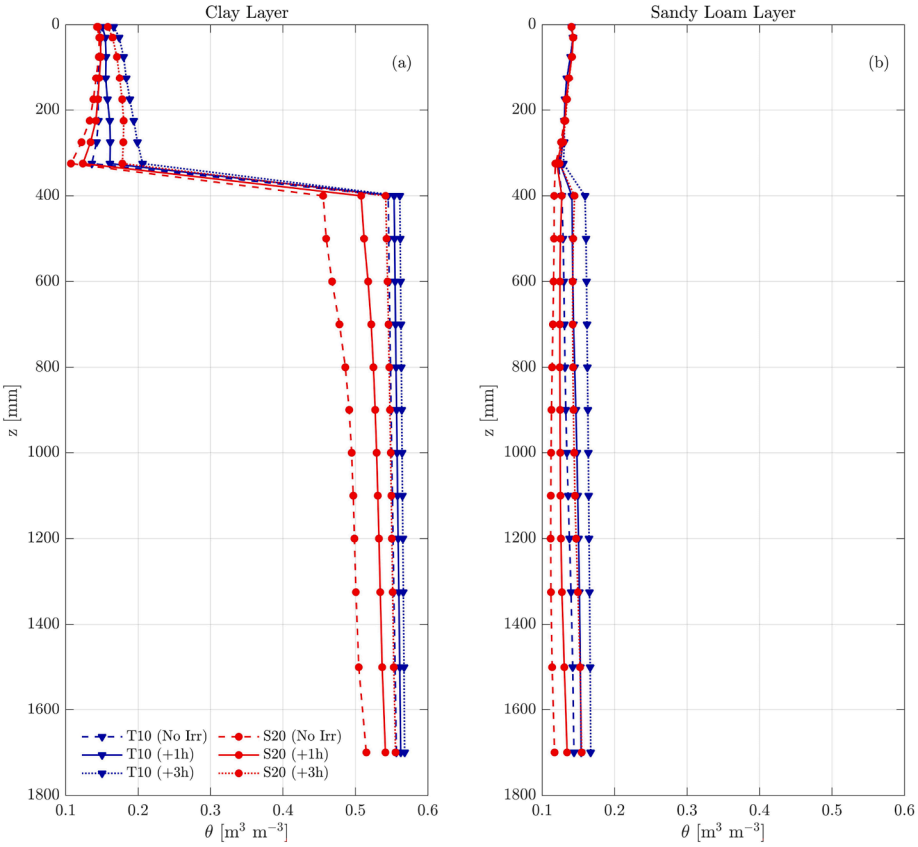

Fig. 5. Changes in vertical profiles of soil moisture. Long-term averaged soil moisture (θ) profile with soil depth for the 10% tree cover scenario (T10) and for the trees-shrubs-grass scenario (S20) with respect to the no irrigation, +1 h irrigation, and +2 h irrigation scenarios. Results correspond to simulations with (a) a clay layer and (b) a sandy loam layer at the bottom of the soil (0.4–1.8 m).

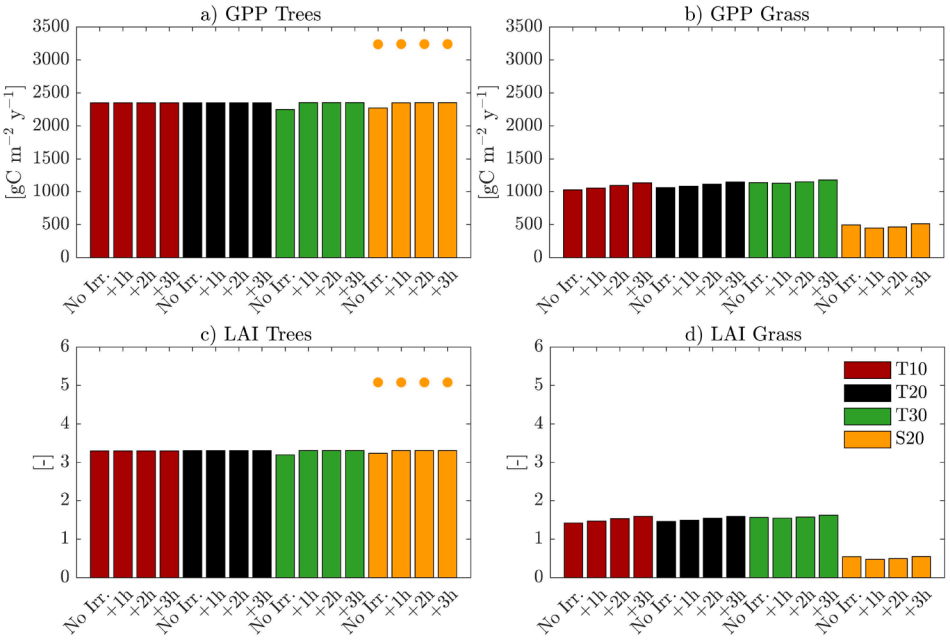

Fig. 6. Simulation results averaged over the 19-year period (July 1999-June 2018) illustrating the sensitivity of vegetation productivity to vegetation cover scenarios (i.e., 10% (T10; red), 20% (T20; black), and 30% (T30; green) tree cover as well as 20% trees, 50% grass, and 20% shrubs cover (S20; orange)), and irrigation scenarios (i.e., No Irrigation, +1 h, +2 h, and +3 h). Gross primary productivity (GPP; for unit of vegetated area) for (a) trees (bars) and shrubs (dots), and (b) grass; leaf area index (LAI; for unit of vegetated area) for (c) trees (bars) and shrubs (dots), and (d) grass.

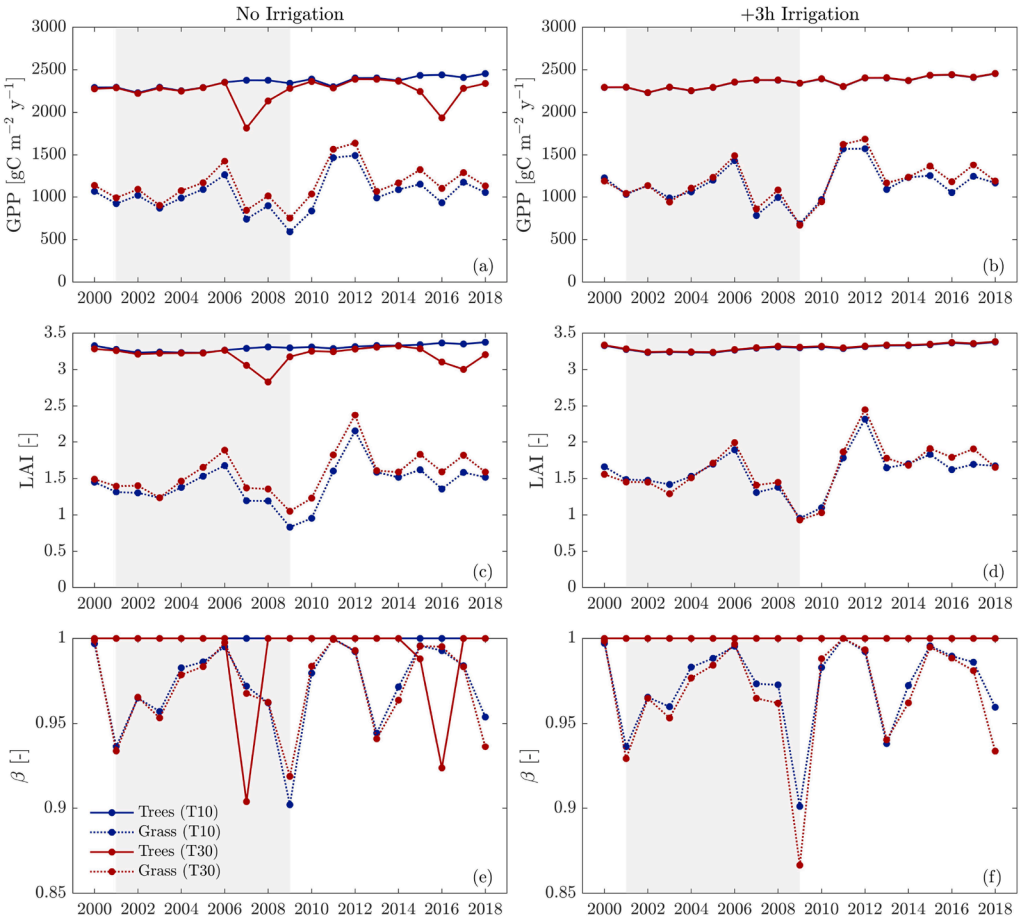

Fig. 7. Simulation results for the 19 year period (July 1999-June 2018) corresponding to tree covers of 10% (T10; blue) and 30% (T30; red) (a, c, e) without irrigation and (b, d, f) for the +3 h irrigation scenario. (a, b) Total annual values of gross primary productivity (GPP; for unit of vegetated area) for trees (GPP^T) and grass (GPP^G). (c, d) Mean annual values of leaf area index (LAI; for unit of vegetated area) for trees (LAI^T) and grass (LAI^G). (e, f) Mean annual values of plant water stress (β=1, unstressed conditions) for trees (β_T) and grass (β_G). Grey regions indicate the period of the Millennium Drought.

grass biomass was more responsive to changes in the water availability and showed a strongly variable LAI during the simulated period in all vegetation cover scenarios, reducing LAI by −37% and −25% in 2009 compared to the beginning of the Millennium Drought (2001) for the 10% and 30% tree cover, respectively (Fig. 7c). The impacts of irrigation were quite pronounced in terms of tree productivity during dry years, especially for the scenario with the 30% tree cover, i.e., +31% in 2007 and +26% in 2016 when irrigation was considered (Fig. 7b).

Shrubs tended to outcompete grass in most conditions, because grass is highly susceptible to water stress (annual average values of β always

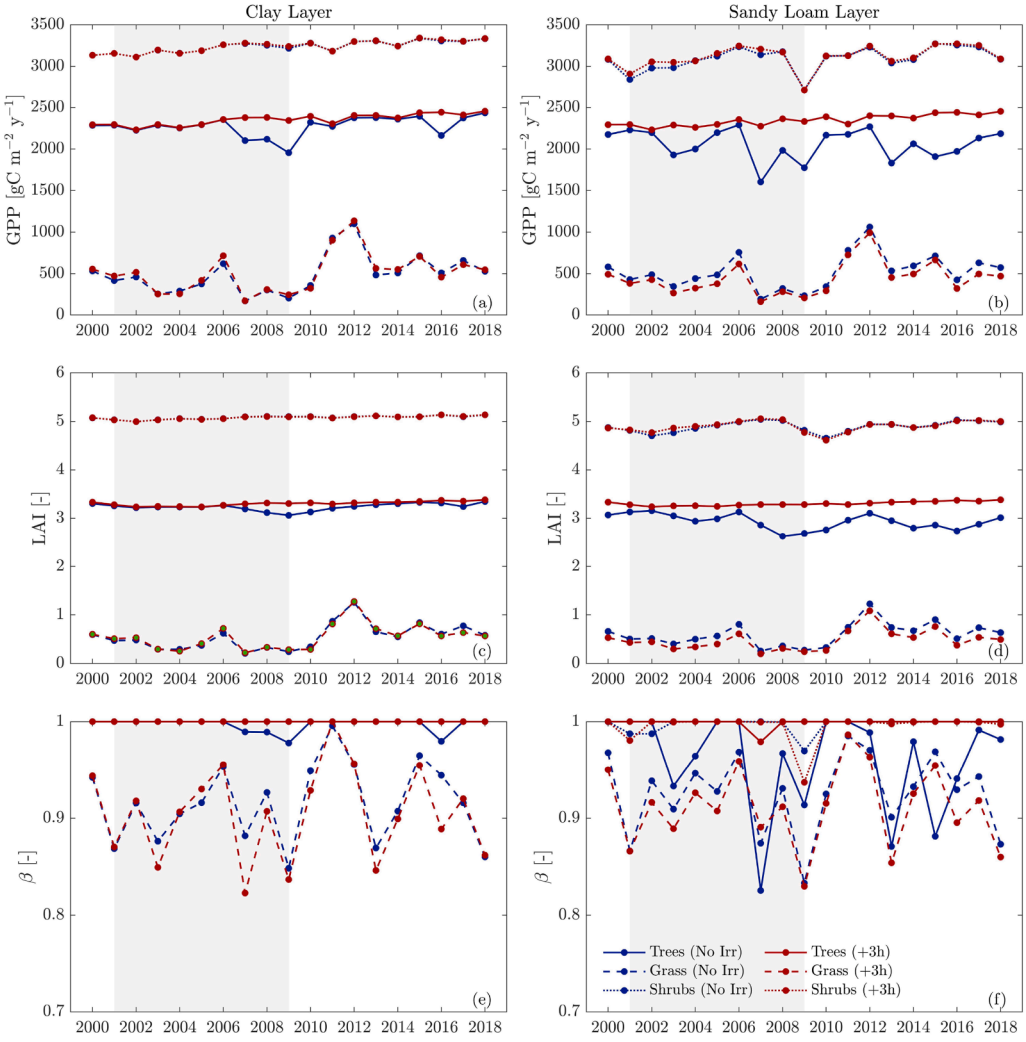

Fig. 8. Simulation results for the 19 year period (July 1999-June 2018) without irrigation corresponding to the scenario that accounts for the coexistence of trees (20%), shrubs (20%), and grass (50%) for both soil types, i.e., (a, c, e) clay and (b, d, f) sandy loam. (a, b) Total annual values of gross primary productivity (GPP; for unit of vegetated area) for trees (GPP^T), grass (GPP^G), and shrubs (GPP^S). (c, d) Mean annual values of leaf area index (LAI; for unit of vegetated area) for trees (LAI^T), grass (LAI^G), and shrubs (LAI^S). (e, f) Mean annual values of plant water stress (β=1, unstressed conditions) for trees (β_T), grass (β_G), and shrubs (β_S). Grey regions indicate the period of the Millennium Drought.

below 1 except for very wet years, i.e., 2011) (Fig. 8e). Trees were also found to be more stressed, showing a decrease in both GPP and LAI between 2007 and 2009 and in 2016 (Figs. 8a and 8c). When accounting for irrigation GPP of trees increased especially with respect to the +3 h irrigation scenario compared to the scenario without irrigation (i.e., +13% in 2007, +12% in 2008, +20% in 2009, and +13% in 2016; Fig. 8a). The presence of a sandy loam layer instead of a clay layer exacerbated the competition for water between woody plants (i.e., trees and shrubs) and grasses, strongly affecting the overall tree productivity (Fig. 8b). In terms of plant water stress, trees were found to be highly susceptible to water stress when irrigation is absent, reaching a minimum value (β=0.83) in 2007; on the contrary, shrubs were overall less stressed than trees when irrigation is absent, with the exception of some years (i.e., 2001 and 2002) (Fig. 8f).

4. Discussion

Results from this study indicate that, if the irrigation system had been in place during the Millennium Drought, it could have helped both the trees and grass by increasing soil moisture. However, the irrigation after the drought seems to have benefited mostly the grass across the reserve. With a tree cover of 10%, simulations showed that trees coped quite well with drought even without irrigation. This is mainly because the trees at Napier Park mostly rely on the water stored in the clay layer within the duplex soil. However, when tree cover was increased, trees were found to be more stressed especially during the driest years. Therefore, increasing the volume of water available by means of irrigating after each rainfall event would have helped a larger tree cover to remain unstressed during the Millennium Drought (Luketich, Papuga, & Crimmins, 2019).

Model results also indicate that the coexistence of trees, shrubs, and grass strongly modifies the competition for water between woody plants (i.e., trees and shrubs) and grasses (Eggemeyer et al., 2009). Differences in terms of rooting depth and tolerance to lower water potentials are critical for plant water access, canopy transpiration, and carbon assimilation. Shallow-rooted grass species only access soil moisture in the shallow soil layers, while trees and shrubs have access to the water in both shallow and deep soil layers (Kim & Eltahir, 2004; Rossatto, Silva, Villalobos-Vega, Sternberg, & Franco, 2012). When shrubs are competing for water resources with both grass and trees, a decline in grass productivity of about −50% was estimated while trees showed small variations in GPP. Grasses wilted reducing their leaf area and became almost inactive during dry periods, whereas trees and shrubs maintained their leaf area when stressed, with a reduction of transpiration via stomata regulation (McDowell et al., 2008). When irrigation was considered, competition was alleviated and GPP of trees increased, especially during the drought period; conversely, GPP of grass did not increase much when shrubs were introduced.

By varying the amount of annual water input in a realistic range for Napier Park, the trajectories of GPP with irrigation indicated that a threshold value for the amount of irrigation needed can be determined, as also found by Volo et al. (2014). Specifically, simulations showed that

a +1 h irrigation scenario (i.e., 98 mm y^{-1}) was sufficient to largely reduce water stress. By adding further water, losses increased mainly through leakage from the bottom of the soil domain and runoff; a slight increase in total evapotranspiration was also found mainly due to an increase in evaporation from bare soil, thus not contributing to additional plant productivity (Figs. 3 and 6). Such results highlight the need for outdoor water use optimization to avoid over-irrigation, especially in arid and semi-arid cities, where there is a trade-off between increasing vegetation productivity and preserving water (Reyes-Paecke, Gironás, Melo, Vicuña, & Herrera, 2019).

The high water holding capacity of clay soil played a crucial role in storing water accessible to the trees. Conversely, when a sandy loam soil was considered, results indicate that most of the water is lost through leakage from the soil bottom, reaching about +66% when a +3 h irrigation scenario was considered with respect to 10% tree cover. When soil is more sandy, the storage capacity becomes insufficient to supply moisture to the woody plants for the entire growing season, affecting their competitive performance. This is intensified by the coexistence of trees, shrubs, and grass, with trees more stressed especially as drought intensified, suggesting that the water status and competitiveness of vegetation may differ significantly depending on the soil type. The clay layer can prevent percolation of water that remains stored in the soil and can support vegetation with deeper root systems through periods of drought, similarly to shallow groundwater resources in urban areas (Marchionni et al., 2019; Marchionni et al., 2020).

The results of this study focus on hydrological fluxes and vegetation dynamics, which are important drivers of ecosystem services in urban environments, such as cooling and carbon sequestration; other ecosystem services, such as recreational aspects, can not be analyzed with the T&C model. In addition, because the results of this study are based on a model calibrated to specific sites with certain climatic conditions, soil properties, and vegetation composition, it would be difficult to transfer these results to other sites without conducting a similar analysis. However, the results are indicative of the general impacts of irrigation with respect to a wider range of vegetation species and compositions; this is especially relevant in arid and semi-arid urban areas, where the coexistence of native and non-native species may create unique biotic communities highly dependent on irrigation. Moreover, in the current model application the exact position of the tree canopies was not considered and the different types of vegetation were not overlapped vertically (i.e., no grass is present under tree canopies). A full treatment of vertically stacked vegetation with an exact tree canopy distribution would require a full 3D scene and 3D solution of canopy radiative transfer, which is beyond the scope of terrestrial biosphere models as T&C and would require a much more detailed description of the urban reserve, which is unlikely often available.

5. Conclusion

By quantifying the impacts of irrigation on hydrological fluxes and vegetation dynamics, this study highlighted the role of water addition using harvested stormwater to help buffer the effects of local rainfall decrease on urban reserves and relatively large urban green spaces. We show that the vegetation cover and soil types needs to be considered when planning and designing irrigation rates. In the analyzed case study, when tree cover is low, irrigation might not be crucial to keep trees healthy, especially if some water stress in grassland can be tolerated. Conversely, an increase in tree cover and the introduction of non-native species may result in higher water demand, thus making irrigation essential to the maintenance of such vegetation. Soil properties play an important role in supporting vegetation water use by defining the ability to store water for evapotranspiration. This highlights the need for a sustainable balance between urban greening, which provides ecosystem services, and water conservation. In this context, mechanistic numerical models represent valuable tools to guide urban planning and for a sustainable design and management of urban green areas.

Declaration of Competing Interest

The authors declare that they have no known competing financial interests or personal relationships that could have appeared to influence the work reported in this paper.

Acknowledgement

VM, ED, NT and JW acknowledge the support of the Australian Research Council, and the City of Greater Dandenong and Mooney Valley City councils through the Linkage project LP150100901. GM acknowledges support by the “The BrancoWeiss Fellowship - Society in Science” administered by ETH Zurich.

Appendix A. Supplementary data

Supplementary data associated with this article can be found, in the online version, athttps://doi.org/10.1016/j.landurbplan.2021.104198.

References

Abram, N. J., Henley, B. J., Gupta, A. S., Lippmann, T. J., Clarke, H., Dowdy, A. J., Sharples, J. J., Nolan, R. H., Zhang, T., Wooster, M. J., et al. (2021). Connections of climate change and variability to large and extreme forest fires in southeast australia. *Communications Earth & Environment, 2*, 1–17.

Allen, C. D., Breshears, D. D., & McDowell, N. G. (2015). On underestimation of global vulnerability to tree mortality and forest die-off from hotter drought in the anthropocene. *Ecosphere, 6*, 1–55.

Allen, M. A., Roberts, D. A., & McFadden, J. P. (2021). Reduced urban green cover and daytime cooling capacity during the 2012–2016 california drought. *Urban Climate, 36*, Article 100768.

Breshears, D. D., Cobb, N. S., Rich, P. M., Price, K. P., Allen, C. D., Balice, R. G., Romme, W. H., Kastens, J. H., Floyd, M. L., Belnap, J., et al. (2005). Regional vegetation die-off in response to global-change-type drought. *Proceedings of the National Academy of Sciences, 102*, 15144–15148.

Breyer, B., Zipper, S. C., & Qiu, J. (2018). Sociohydrological impacts of water conservation under anthropogenic drought in Austin, TX (USA). *Water Resources Research, 54*, 3062–3080.

Broadbent, A. M., Coutts, A. M., Tapper, N. J., & Demuzere, M. (2018). The cooling effect of irrigation on urban microclimate during heatwave conditions. *Urban Climate, 23*, 309–329.

Calfapietra, C., Peñuelas, J., & Niinemets, Ü. (2015). Urban plant physiology: adaptation-mitigation strategies under permanent stress. *Trends in Plant Science, 20*, 72–75.

Carsel, R. F., & Parrish, R. S. (1988). Developing joint probability distributions of soil water retention characteristics. *Water Resources Research, 24*, 755–769.

Chiesura, A. (2004). The role of urban parks for the sustainable city. *Landscape and Urban Planning, 68*, 129–138.

Collins, D., & Bras, R. (2007). Plant rooting strategies in water-limited ecosystems. *Water Resources Research, 43*.

De Kauwe, M. G., Medlyn, B. E., Ukkola, A. M., Mu, M., Sabot, M. E., Pitman, A. J., Meir, P., Cernusak, L. A., Rifai, S. W., Choat, B., et al. (2020). Identifying areas at risk of drought-induced tree mortality across south-eastern australia. *Global Change Biology, 26*, 5716–5733.

van Dijk, A. I., Beck, H. E., Crosbie, R. S., de Jeu, R. A., Liu, Y. Y., Podger, G. M., Timbal, B., & Viney, N. R. (2013). The Millennium Drought in southeast Australia (2001–2009): Natural and human causes and implications for water resources, ecosystems, economy, and society. *Water Resources Research, 49*, 1040–1057.

Eggemeyer, K. D., Awada, T., Harvey, F. E., Wedin, D. A., Zhou, X., & Zanner, C. W. (2009). Seasonal changes in depth of water uptake for encroaching trees juniperus virginiana and pinus ponderosa and two dominant c4 grasses in a semiarid grassland. *Tree Physiology, 29*, 157–169.

Elmqvist, T., Setälä, H., Handel, S., Van Der Ploeg, S., Aronson, J., Blignaut, J. N., Gomez-Baggethun, E., Nowak, D., Kronenberg, J., & De Groot, R. (2015). Benefits of restoring ecosystem services in urban areas. *Current Opinion in Environmental Sustainability, 14*, 101–108.

Entekhabi, D., Yueh, S., O'Neill, P.E., Kellogg, K.H., Allen, A., Bindlish, R., Brown, M., Chan, S., Colliander, A., Crow, W.T., et al., 2014. Smap handbook–soil moisture active passive: Mapping soil moisture and freeze/thaw from space.

Fatichi, S., Ivanov, V., & Caporali, E. (2012). A mechanistic ecohydrological model to investigate complex interactions in cold and warm water-controlled environments: 1. theoretical framework and plot-scale analysis. *Journal of Advances in Modeling Earth Systems, 4*.

Fatichi, S., & Pappas, C. (2017). Constrained variability of modeled T:ET ratio across biomes. *Geophysical Research Letters, 44*, 6795–6803.

Fatichi, S., Zeeman, M. J., Fuhrer, J., & Burlando, P. (2014). Ecohydrological effects of management on subalpine grasslands: From local to catchment scale. *Water Resources Research, 50*, 148–164.

Flörke, M., Schneider, C., & McDonald, R. I. (2018). Water competition between cities and agriculture driven by climate change and urban growth. *Nature Sustainability, 1*, 51–58.

Gill, S. E., Handley, J. F., Ennos, A. R., & Pauleit, S. (2007). Adapting cities for climate change: the role of the green infrastructure. *Built environment, 33*, 115–133.
Kim, Y., & Eltahir, E. A. (2004). Role of topography in facilitating coexistence of trees and grasses within savannas. *Water Resources Research, 40*.
Kleinschroth, F., & Kowarik, I. (2020). Covid-19 crisis demonstrates the urgent need for urban greenspaces. *Frontiers in Ecology and the Environment, 18*, 318.
Lepczyk, C. A., Aronson, M. F., Evans, K. L., Goddard, M. A., Lerman, S. B., & MacIvor, J. S. (2017). Biodiversity in the city: Fundamental questions for understanding the ecology of urban green spaces for biodiversity conservation. *BioScience, 67*, 799–807.
Litvak, E., & Pataki, D. E. (2016). Evapotranspiration of urban lawns in a semi-arid environment: An in-situ evaluation of microclimatic conditions and watering recommendations. *Journal of Arid Environments, 134*, 87–96.
Livesley, S., McPherson, E. G., & Calfapietra, C. (2016). The urban forest and ecosystem services: impacts on urban water, heat, and pollution cycles at the tree, street, and city scale. *Journal of environmental quality, 45*, 119–124.
Livesley, S. J., Marchionni, V., Cheung, P. K., Daly, E., & Pataki, D. E. (2020). Water smart cities increase irrigation to provide cool refuge in a climate crisis. Earth's. *Future, e2020EF001806*.
Low, K. G., Grant, S. B., Hamilton, A. J., Gan, K., Saphores, J. D., Arora, M., & Feldman, D. L. (2015). Fighting drought with innovation: Melbourne's response to the millennium drought in southeast australia. *Wiley Interdisciplinary Reviews: Water, 2*, 315–328.
Luederitz, C., Brink, E., Gralla, F., Hermelingmeier, V., Meyer, M., Niven, L., Panzer, L., Partelow, S., Rau, A. L., Sasaki, R., et al. (2015). A review of urban ecosystem services: six key challenges for future research. *Ecosystem services, 14*, 98–112.
Luketich, A. M., Papuga, S. A., & Crimmins, M. A. (2019). Ecohydrology of urban trees under passive and active irrigation in a semiarid city. *PloS one, 14*, Article e0224804.
Manoli, G., Ivanov, V. Y., & Fatichi, S. (2018). Dry-season greening and water stress in amazonia: The role of modeling leaf phenology. *Journal of Geophysical Research: Biogeosciences, 123*, 1909–1926.
Manoli, G., Meijide, A., Huth, N., Knohl, A., Kosugi, Y., Burlando, P., Ghazoul, J., & Fatichi, S. (2018). Ecohydrological changes after tropical forest conversion to oil palm. *Environmental Research Letters, 13*, Article 064035.
Marchionni, V., Daly, E., Manoli, G., Tapper, N., Walker, J., & Fatichi, S. (2020). Groundwater buffers drought effects and climate variability in urban reserves. *Water Resources Research, 56*, Article e2019WR026192.
Marchionni, V., Guyot, A., Tapper, N., Walker, J., & Daly, E. (2019). Water balance and tree water use dynamics in remnant urban reserves. *Journal of Hydrology, 575*, 343–353.
Marchionni, V., Revelli, R., & Daly, E. (2019). Ecohydrology of urban ecosystems. In *Dryland Ecohydrology* (pp. 533–571). Springer.
Martire, J.L., 2018. Stormwater reuse for parks and whole cities. ReNew: Technology for a Sustainable Future, 72–75.
Mastrotheodoros, T., Pappas, C., Molnar, P., Burlando, P., Hadjidoukas, P., & Fatichi, S. (2019). Ecohydrological dynamics in the Alps: Insights from a modelling analysis of the spatial variability. *Ecohydrology, 12*, Article e2054.
McCarthy, H. R., & Pataki, D. E. (2010). Drivers of variability in water use of native and non-native urban trees in the greater Los Angeles area. *Urban Ecosystems, 13*, 393–414.
McCarthy, H. R., Pataki, D. E., & Jenerette, G. D. (2011). Plant water-use efficiency as a metric of urban ecosystem services. *Ecological Applications, 21*, 3115–3127.
McDowell, N., Pockman, W. T., Allen, C. D., Breshears, D. D., Cobb, N., Kolb, T., Plaut, J., Sperry, J., West, A., Williams, D. G., et al. (2008). Mechanisms of plant survival and mortality during drought: why do some plants survive while others succumb to drought? *New phytologist, 178*, 719–739.
Mcdowell, N. G., Williams, A., Xu, C., Pockman, W., Dickman, L., Sevanto, S., Pangle, R., Limousin, J., Plaut, J., Mackay, D., et al. (2016). Multi-scale predictions of massive conifer mortality due to chronic temperature rise. *Nature Climate Change, 6*, 295.
McPherson, G.E., Simpson, J.R., Xiao, Q., Chunxia, W., 2008. Los angeles 1-million tree canopy cover assessment. Gen. Tech. Rep. PSW-GTR-207. Albany, CA: US Department of Agriculture, Forest Service, Pacific Southwest Research Station. 52 p 207.
Meili, N., Manoli, G., Burlando, P., Carmeliet, J., Chow, W. T., Coutts, A. M., Roth, M., Velasco, E., Vivoni, E. R., & Fatichi, S. (2020). Tree effects on urban microclimate: diurnal, seasonal, and climatic temperature differences explained by separating radiation, evapotranspiration, and roughness effects. *Urban Forestry & Urban Greening, 126970*.
Melbourne, 2012. Urban forest strategy: Making a great city greener 2012–2032.
Miller, D. L., Alonzo, M., Roberts, D. A., Tague, C. L., & McFadden, J. P. (2020). Drought response of urban trees and turfgrass using airborne imaging spectroscopy. *Remote Sensing of Environment, 240*, Article 111646.
Nouri, H., Borujeni, S. C., & Hoekstra, A. Y. (2019). The blue water footprint of urban green spaces: An example for Adelaide. *Australia. Landscape and urban planning, 190*, Article 103613.
Pataki, D., Boone, C., Hogue, T., Jenerette, G., McFadden, J., & Pincetl, S. (2011). Socio-ecohydrology and the Urban Water Challenge. *Ecohydrology, 4*, 341–347.
Pataki, D. E., Carreiro, M. M., Cherrier, J., Grulke, N. E., Jennings, V., Pincetl, S., Pouyat, R. V., Whitlow, T. H., & Zipperer, W. C. (2011). Coupling biogeochemical cycles in urban environments: ecosystem services, green solutions, and misconceptions. *Frontiers in Ecology and the Environment, 9*, 27–36.
Qiu, J., Zipper, S. C., Motew, M., Booth, E. G., Kucharik, C. J., & Loheide, S. P. (2019). Nonlinear groundwater influence on biophysical indicators of ecosystem services. *Nature Sustainability, 2*, 475.
Quesnel, K. J., Ajami, N., & Marx, A. (2019). Shifting landscapes: decoupled urban irrigation and greenness patterns during severe drought. *Environmental Research Letters, 14*, Article 064012.
Reyes-Paecke, S., Gironás, J., Melo, O., Vicuña, S., & Herrera, J. (2019). Irrigation of green spaces and residential gardens in a Mediterranean metropolis: Gaps and opportunities for climate change adaptation. *Landscape and Urban Planning, 182*, 34–43.
Richards, L. A. (1931). Capillary conduction of liquids through porous mediums. *Physics, 1*, 318–333.
Roberts, B. R. (1977). The response of urban trees to abiotic stress [moisture, temperature, light, pesticides]. *Journal of Arboriculture (USA)*.
Rossatto, D.R., Silva, L.d.C.R., Villalobos-Vega, R., Sternberg, L.d.S.L., Franco, A.C., 2012. Depth of water uptake in woody plants relates to groundwater level and vegetation structure along a topographic gradient in a neotropical savanna. Environmental and Experimental Botany 77, 259–266.
Sawada, Y., & Koike, T. (2016). Ecosystem resilience to the Millennium drought in southeast Australia (2001–2009). *Journal of Geophysical Research: Biogeosciences, 121*, 2312–2327.
Sieghardt, M., Mursch-Radlgruber, E., Paoletti, E., Couenberg, E., Dimitrakopoulus, A., Rego, F., Hatzistathis, A., & Randrup, T. B. (2005). The abiotic urban environment: impact of urban growing conditions on urban vegetation. *Springer.*, 281–323.
Soylu, M., Istanbulluoglu, E., Lenters, J., & Wang, T. (2011). Quantifying the impact of groundwater depth on evapotranspiration in a semi-arid grassland region. *Hydrology and Earth System Sciences, 15*, 787–806.
Spronken-Smith, R., & Oke, T. (1998). The thermal regime of urban parks in two cities with different summer climates. *International Jurnal of Remote Sensing, 19*, 2085–2104.
Tulloch, A. I., Barnes, M. D., Ringma, J., Fuller, R. A., & Watson, J. E. (2016). Understanding the importance of small patches of habitat for conservation. *Journal of Applied Ecology, 53*, 418–429.
Van Genuchten, M. T. (1980). A closed-form equation for predicting the hydraulic conductivity of unsaturated soils 1. *Soil Science Society of America Journal, 44*, 892–898.
Volo, T. J., Vivoni, E. R., Martin, C. A., Earl, S., & Ruddell, B. L. (2014). Modelling soil moisture, water partitioning, and plant water stress under irrigated conditions in desert urban areas. *Ecohydrology, 7*, 1297–1313.
Wallace, P. (2014). City of melbourne to reap its harvest. *Waste Management and Environment, 25*, 22–23.